

Comparison of retrospective PET and MRI-DWI (PET/MRI-DWI) image fusion with PET/CT and MRI-DWI in detection of cervical and endometrial cancer lymph node metastases

Alessandro Stecco¹ · Francesco Buemi¹ · Alessia Cassarà¹ · Roberta Matheoud² · Gian Mauro Sacchetti³ · Alberto Arnulfo⁴ · Marco Brambilla² · Alessandro Carriero¹

Received: 15 May 2015 / Accepted: 26 January 2016 / Published online: 31 March 2016
© Italian Society of Medical Radiology 2016

Abstract

Objectives The aim of this study was to compare the accuracy of retrospective image fusion of PET/MRI-DWI with that of PET/CT and MRI-DWI alone in detecting metastatic lymph nodes in patients with cervical and endometrial carcinoma.

Materials and methods Twenty-seven patients with endometrial ($n = 14$) and cervical ($n = 13$) cancer who had undergone preoperative MRI-DWI and PET/CT for staging were retrospectively evaluated. The accuracy, sensitivity, specificity, positive predictive value (PPV), and negative predictive value (NPV) of PET/CT, MRI-DWI, and PET/MRI-DWI image fusion were calculated on a per-patient basis and on a per-node basis. Histopathological and follow-up imaging results were used as the gold standard.

Results On a per-patient basis PET/MRI-DWI had the same sensitivity (87.5 %), specificity (84.2 %), diagnostic accuracy (85.1 %), PPV (70 %), and NPV (94.1 %) as PET-CT, but on a per-node basis PET/MRI-DWI showed better sensitivity (89 vs 70.2 %), specificity (91.6 vs 90.5 %), diagnostic accuracy (91.2 vs 87 %), PPV (68.7 vs 60.4 %), and NPV (97.6 vs 93.6 %) than PET-CT. Comparison of the

areas under the ROC curves for the detection of metastatic lymph nodes demonstrated a non-significant difference ($p = 0.055$) between PET/CT and fused PET/MRI-DWI.

Conclusion PET/MRI-DWI may be a valuable technique for N-staging patients with endometrial and cervical cancer, but more studies are needed to investigate its potential clinical utility.

Keywords PET/CT · DWI · MRI · Fusion Imaging · Uterine cancer

Introduction

The International Federation of Gynecology and Obstetrics (FIGO) system is the most widely used for staging uterine cervical and endometrial cancer [1]. However, the FIGO staging system does not take into account lymph node (LN) metastasis (so-called N staging), despite its known adverse impact on survival in gynecological cancer [2, 3]. Although LN resection before radiotherapy results in improved survival in patients with macroscopically enlarged pelvic and para-aortic LNs, routine pre-surgical staging is not generally recommended, even though a lack of assessment of LN involvement may lead to suboptimal treatment [4–9].

Indeed, the gold standard for diagnosing LN metastases is currently surgical assessment [10], but this is a highly specialized, time-consuming, costly and invasive procedure that increases the patient's risk of immediate and delayed complications. Hence, a non-invasive but accurate pre-surgical method of diagnosing LN metastases would be desirable, helping to prevent unnecessary lymphadenectomy and optimizing surgical interventions. In this context, computed tomography (CT) and magnetic resonance imaging (MRI) are widely used to assess LNs in patients with malignant

✉ Alessandro Stecco
a.stecco@libero.it

¹ Radiology Department, University of Eastern Piedmont, "Maggiore della Carità" Hospital, Corso Mazzini 18, 28100 Novara, Italy

² Medical Physics Department, University of Eastern Piedmont, "Maggiore della Carità" Hospital, Novara, Italy

³ Nuclear Medicine Department, University of Eastern Piedmont, "Maggiore della Carità" Hospital, Novara, Italy

⁴ Gynecology Department, University of Eastern Piedmont, "Maggiore della Carità" Hospital, Novara, Italy

tumors, including uterine cancer. As the state of the art progresses, various functional imaging techniques, including diffusion-weighted MRI (MRI-DWI), and combined positron emission tomography and CT (PET/CT) using 18F-fluoro-deoxy-glucose (FDG), have been proposed as a method of improving diagnostic performance.

To date, there have been three reports on apparent diffusion coefficient (ADC) obtained with DWI for the detection of LN metastasis [11–13], and several on PET/CT [14–20] for uterine cancer. PET/MRI image fusion is increasingly being used in clinical settings, although both clinical evaluation and technical optimization are still developing processes. Nevertheless, initial experience with this new imaging device proves promising for oncological applications [21]. Generally, there are two major image fusion techniques available, namely hardware based and retrospective software based. Hardware-based image fusion is performed by means of hybrid scanners, which enable the real-time acquisition and fusion of two different imaging modalities within a single device. Retrospective software-based image fusion, on the other hand, relies on dedicated software to fuse two separate imaging datasets, most often from CT or MRI and single-photon emission tomography (SPECT) or PET. This technique, called “image registration”, is used to align both sets of data so that each voxel corresponds to the same anatomical landmarks in both images [22].

As yet, however, there have been few studies [23, 24] on the ability of fused PET/MRI imaging to identify metastatic LNs in patients with uterine endometrial and cervical cancer. The purpose of this study was, therefore, to assess the accuracy of retrospective image fusion PET/MRI-DWI to PET/CT in detecting metastatic LNs in patients with newly diagnosed cervical and endometrial carcinoma, comparing PET/MRI-DWI findings with those of both PET/CT and MRI-DWI alone.

Materials and methods

Patients

This retrospective study involved 27 untreated female patients with either endometrial ($n = 14$) or cervical cancer ($n = 13$) (demographic and clinical data are reported in Tables 1, 2, 3) from October 2011 to December 2013. Exclusion criteria were general contraindications for MRI (such as cardiac pacemaker and claustrophobia). Each patient underwent MRI-DWI and PET/CT before undergoing subtotal hysterectomy ($n = 1$), total abdominal hysterectomy with ($n = 8$) or without ($n = 18$) bilateral salpingo-oophorectomy, and pelvic lymphadenectomy, with ($n = 15$) or without ($n = 12$) para-aortic lymphadenectomy, for histopathologically proven uterine cancer. Each

Table 1 Demographic and clinical characteristics of the study population

Number of patients	27
Mean age	56.25
Age range	30–78
SD	13.70
Median	54
Mode	47
Frequency of cervix cancer (%)	13 (48)
Treatment after surgery	
Chemotherapy	5
Chemo-radiotherapy	2
Response to treatment	
Complete remission	8
Recurrence	5
One bone metastasis (CT), two pelvic nodal metastasis (PET/CT and MRI), one peritoneal carcinomatosis (CT), one para-aortic nodal metastasis (CT)	
Frequency of endometrium cancer (%)	14 (52)
Treatment after surgery	
Chemotherapy	6
Chemo-radiotherapy	0
Response to treatment	
Complete remission	11
Recurrence	3
One mesenteric nodal mass (CT and PET/CT), one pelvic nodal metastasis (PET/CT), one bone and right adrenal metastasis (PET/CT)	

Table 2 Frequency and percentage of tumor histotype of the study population

Frequency of cervix cancer	<i>N</i> (%)
Spinocellular carcinoma G2	3 (23)
Spinocellular carcinoma G3	5 (38)
Adenocarcinoma G2	1 (8)
Adenocarcinoma G3	2 (15)
Neuroendocrine carcinoma G2	1 (8)
Squamocellular carcinoma G3	1 (8)
Total	13 (100)
Frequency of endometrium cancer	
Adenocarcinoma G2	2 (14)
Adenocarcinoma G3	5 (36)
Endometrioid carcinoma G2	5 (36)
CIN 3	1 (7)
Leiomyosarcoma G3	1 (7)
Total	14 (100)

pelvic LN was analyzed by a histopathologist. None of the patients had either contraindications to the surgical procedure or clinical evidence of distant metastases.

Table 3 Frequency and percentage of FIGO classification of the study population

FIGO STADIATION of cervix cancer	N (%)
Tis	0 (0)
FIGO IA	0 (0)
FIGO IB	0 (0)
FIGO IIA	0 (0)
FIGO IIB	3 (23)
FIGO IIIA	1 (8)
FIGO IIIB	8 (61)
FIGO IVA	1 (8)
FIGO IVB	0 (0)
Total	13 (100)
FIGO STADIATION of endometrium cancer	
Tis	1 (7)
FIGO IA	1 (7)
FIGO IB	0 (0)
FIGO IIA	0 (0)
FIGO IIB	4 (29)
FIGO IIIA	6 (43)
FIGO IIIB	1 (7)
FIGO IVA	1 (7)
FIGO IVB	0 (0)
Total	14 (100)

Prior to the surgery, four of the patients with cervical cancer underwent an abdominal CT scan in the emergency room. Three had bilateral (one case with severe renal failure) and one unilateral ureter infiltration by the tumor. The time interval between MRI scan and surgical treatment was 5–29 days (mean: 17 days). The time interval between PET/CT scan and surgical treatment was 3–33 days (mean: 18 days). The time interval between MRI scan and PET/CT scan was 0–33 days (mean: 10 days).

Subsequently, 11 patients received chemotherapy alone and 2 chemo-radiotherapy. Women were followed up according to the protocol of our institution. Of the treated patients, 19 achieved complete remission and 8 had recurrent disease (Table 1). Informed consent was obtained from all participants. As the study was retrospective, approval of the local ethics committee was not sought.

PET/CT imaging

Whole body PET/CT images were obtained using a PET/CT scanner Biograph 16 HI-REZ (Siemens, Hoffman Estates, IL). After an 8-h fast, patients received an intravenous injection of 250 MBq FDG, and were encouraged to rest. PET/CT scanning from the middle of the skull to the upper thigh was performed 60 min after the injection. Specifically, a low-dose spiral CT scan was performed using the following

parameters: 120 kV, 33 mA, 1.5 s rotation time, 24 mm collimation and 48 mm table feed per rotation with arms raised, followed by PET image acquisition (2–4 min per bed position three-dimensional acquisition mode, according to the body max index). CT images were reconstructed onto a 512×512 matrix and converted into 511 kiloelectron volt (keV)-equivalent attenuation factors for attenuation correction. PET images were reconstructed onto a 128×128 matrix using the attenuation-weighted Fourier rebinning (FORE-OSEM) iterative reconstruction, with two iterations and eight subsets, and a post-reconstruction Gaussian volume filter with FWHM = 4 mm. PET, PET/CT, and CT images were analyzed using a dedicated Leonardo workstation (Siemens Medical Solutions). The processed images were displayed in coronal, transverse, and sagittal planes.

MR imaging

All patients were scanned using a 1.5-Tesla MRI scanner (Achieva Intera 1.5 T, Philips Medical Solutions, The Netherlands). Pelvic MR images were acquired using a body-sense four-channel phased array pelvic coil for signal reception, with a parallel factor of 1.2, as follows: axial T2-weighted turbo-spin-echo SPAIR images (TR/TE: 4760/100 ms, slice thickness/intersection gap: 3/1 mm, echo train length: 11, matrix: 560×560 , FOV: $432 \text{ mm} \times 432 \text{ mm}$). Axial DWI was performed during free breathing using a Stejskal–Tanner spin-echo echo-planar imaging sequence and a body synergy four-channel coil with parallel factor of zero at the following parameters: TR/TE: 8160/73 ms; flip angle: 90° ; NEX: 6; readout bandwidth: 2369.3 Hz/pixel; matrix: 384×384 ; FOV: $370 \text{ mm} \times 370 \text{ mm}$; and slice thickness/gap: 5/0 mm, *b* values: 0 and 800 s/mm^2 .

Image analysis

All PET and MRI series were retrospectively and manually fused using dedicated image-fusion software, available on the Leonardo multimodality workstation (Siemens Medical Solutions). MR and PET/CT images were stored in a shared database, and the MR images (T2 and DWI) were co-registered to CT images of PET using a semi-automatic voxel-based algorithm. After image registration, the co-registered images were reconstructed and visualized in the axial plane. Alignment was assessed by checking the body outline and the position of motionless metabolically active organs (bone and spine) in all three planes (axial, coronal, and sagittal). When accurate image fusion was not feasible, PET-MRI fusion was evaluated by assessing PET/MRI-DWI-fused images side-by-side with PET and MRI images. PET/CT images were interpreted by a nuclear physician (MS, 17 years experience) and MR images by an abdominal radiologist (AS, 15 years experience). Both

readers were informed of patient history, but blinded to the presence or absence of LN metastases. On DWI images, LNs were classified as cancer positive in the presence of focally abnormal signal intensity higher than the signal intensity of the spinal cord in a location corresponding to the LN chains on T2-weighted images. As ADC value differentiation of LNs in uterine cancer is reportedly controversial [11, 12], LNs in our series were classified on the basis of visual DWI criteria, irrespective of either ADC value or size. On PET/CT and fused PET/MR images, LNs were classed as cancer positive in the presence of either focally appreciable metabolic activity above that of normal muscle, or asymmetric metabolic activity greater than that of normal-appearing LNs at the same level in the contralateral pelvis in a location corresponding to the LN chains on the CT or MR images, respectively [18]. In contrast, LNs with a central unenhanced area suggestive of a fatty hilum were considered benign. As in a previous study [14], LNs were grouped according to anatomical landmarks into eight regions: right common iliac, left common iliac, right external iliac, left external iliac, right internal iliac, left internal iliac, right obturator fossa, and left obturator fossa.

PET/CT and fused PET/MRI-DWI images were interpreted visually using a five-point scoring system as follows: 0 = negative findings, 1 = insignificant yet visible lesion, 2 = equivocal, needs further follow-up, 3 = probably metastasis, 4 = significant metastasis [25, 26]. We created a score sheet (Excel, Microsoft, US) for each patient to enable evaluation of LN region involvement by PET/CT and MRI exams, grids of *N* parameters, imaging techniques (MRI-DWI, PET/CT, PET/MRI), and histopathological data. Scores were given per-patient and per-node basis. Images were examined directly on a computer workstation screen.

Statistical analysis

Sensitivity, specificity, accuracy, and positive and negative predictive values were calculated for each diagnostic method on a per-patient basis and on a per-node basis, adopting histopathological and follow-up imaging (CT, MRI, and PET/CT) results as the gold standard. A receiver operating characteristic (ROC) curve was used to evaluate the diagnostic value of PET/CT, MRI-DWI and PET/MRI-DWI. A *P* value <0.05 was regarded as statistically significant. MedCalc software (MedCalc Software, Belgium) was used to perform all statistical analyses.

Results

LN metastases were identified by histopathology in 8 of 27 patients (29 %), specifically in 37 of the 216 LN regions (17 %) examined.

Findings on a per-patient basis

DWI was true positive for nodal metastases in 7/8 (87 %) of patients with LN metastases, and true negative for 13/19 (68 %) of patients without node metastases. Similarly, PET/CT and PET/MRI-DWI were true positive for nodal metastases in 7/8 (87 %) of patients with node metastasis, but true negative in 16/19 (84 %) of patients without node metastasis (Table 4). DWI alone showed 87.5 % sensitivity, 68.4 % specificity, 74 % diagnostic accuracy, 53.8 % positive predictive value (PPV), and 92.8 % negative predictive value (NPV). PET-CT and fused PET/MRI-DWI showed 87.5 % sensitivity, 84.2 % specificity, 85.1 % diagnostic accuracy, 70 % PPV, and 94.1 % NPV (Table 4).

The area under the ROC curve (AUC) of PET/CT was 0.859 (confidence interval; 0.710–1.000), while MRI-DWI and PET-MRI AUCs were, respectively, 0.780 (0.617–0.942) and 0.859 (0.710–1.000) (Fig. 1).

Findings on a per-node basis

The LN regions bearing metastases were the common iliac (*n* = 8), external iliac (*n* = 8), internal iliac (*n* = 8), and the obturator fossa (*n* = 13). DWI was true positive for 32 of the 37 (86 %) metastatic node groups, and true negative for 119 of the 179 (66 %) non-metastatic node groups. PET/CT was true positive for 26 of the 37 (70 %) metastatic node groups, and true negative for 162 of the 179 (90 %) non-metastatic node groups. PET/MRI-DWI fared better, being true positive for 33 of the 37 (89 %) metastatic node groups and true negative for 164 of the 179 (91 %) non-metastatic node groups.

Table 4 Parameters of diagnostic performance including FP, FN, TP, TN, sensitivity, specificity. Accuracy, PPV, and NPV of DWI, PET/CT and PET/MRI-DWI on a per-patient basis

	DWI-MRI	PET/CT	PET/MRI-DWI
TP	7	7	7
TN	13	16	16
FP	6	3	3
FN	1	1	1
Sensitivity	87.5 % (CI 47.3–99.6 %)	87.5 % (CI 47.3–99.6 %)	87.5 % (CI 47.3–99.6 %)
Specificity	68.4 % (CI 43.4–87.4 %)	84.2 % (CI 60.4–96.6 %)	84.2 % (CI 60.4–96.6 %)
Accuracy	74 % (CI 57.5–90.6 %)	85.1 % (CI 71.7–98.5 %)	85.1 % (CI 71.7–98.5 %)
PPV	53.8 % (CI 25.1–80.7 %)	70 % (CI 34.7–93.3 %)	70 % (CI 34.7–93.3 %)
NPV	70 % (CI 34.7–93.3 %)	94.1 % (CI 71.3–99.8 %)	94.1 % (CI 71.3–99.8 %)

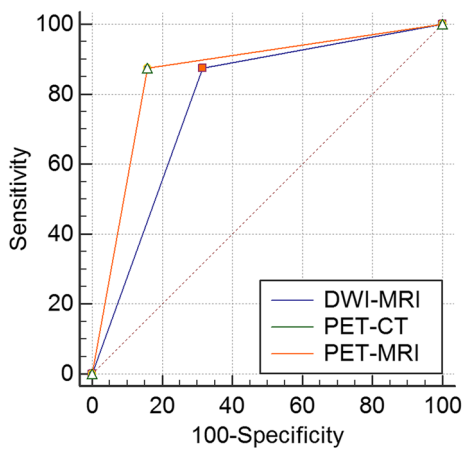


Fig. 1 Graphs of ROC analysis “on a per patient basis”. *Green line*, PET/CT images; *blue line*, DWI-MRI images; *orange line*, fused PET/MRI-DWI images. The area under the ROC curve (AUC) of PET/CT was 0.859 (0.710–1.000), while DWI-MRI and PET-MRI AUCs were 0.780 (0.617–0.942), and 0.859 (0.710–1.000)

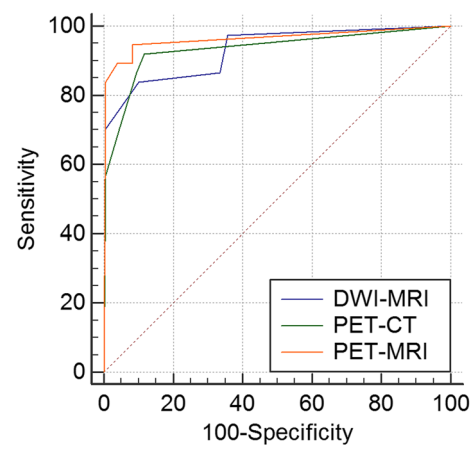


Fig. 2 Graphs of ROC analysis “on a per node basis”. *Green line*, PET/CT images; *blue line*, DWI-MRI images; *orange line* fused PET/MRI-DWI images. The AUC of PET/CT was 0.933 (0.891–0.962), while DWI-MRI and PET-MRI AUCs were 0.929 (0.886–0.960) and 0.963 (0.928–0.984), respectively

Table 5 Parameters of diagnostic performance including FP, FN, TP, TN, sensitivity, specificity. Accuracy, PPV and NPV of DWI, PET/CT, and PET/MRI-DWI on a per-node basis

	MRI-DWI	PET/CT	PET/MRI-DWI
TP	32	26	33
TN	119	162	164
FP	60	17	15
FN	5	11	4
Sensitivity	86.4 % (CI 71.2–95.4 %)	70.2 % (CI 53–84.1 %)	89.1 % (CI 74.5–96.9 %)
Specificity	66.4 % (CI 59–73.3 %)	90.5 % (CI 85.2–94.3 %)	91.6 % (CI 88.5–95.2 %)
Accuracy	69.9 % (CI 63.7–76 %)	87 % (CI 82.5–91.5 %)	91.2 % (CI 87.4–94.9 %)
PPV	91.2 % (CI 87.4–94.9 %)	60.4 % (CI 44.4–75 %)	68.7 % (CI 53.7–81.3 %)
NPV	95.9 % (90.8–98.6 %)	93.6 % (CI 88.9–96.7 %)	97.6 % (CI 94–99.3 %)

Across node groups, DWI alone displayed 86.4 % sensitivity, 66.4 % specificity, 69.9 % diagnostic accuracy, 34.7 % PPV, and 95.9 % NPV, respectively.

The sensitivity, specificity, accuracy, PPV and NPV of PET-CT vs PET/MRI-DWI for the detection of pelvic metastatic LNs were 70.2 vs 89.1 %, 87 vs 91.6 %, 87 vs 91.2 %, 60.4 vs 68.7 %, and 93.6 vs 97.6 %, respectively (Table 5).

The AUC of PET/CT was 0.933 (0.891–0.962), while MRI-DWI and PET/MRI AUCs were 0.929 (0.886–0.960) and 0.963 (0.928–0.984), respectively (Fig. 2). Comparison of the areas under the ROC curves for the detection of metastatic LNs revealed, however, that the difference between PET/CT and fused PET/MRI-DWI was not significant ($p = 0.055$).

Discussion

A non-invasive technique that can accurately identify LN metastasis in malignant tumors would be beneficial for optimizing treatment management. The identification of metastatic LNs by both CT and MRI is based on measurements of node size, and the most widely accepted criterion for diagnosis of nodal involvement, a short-axis diameter greater than 8–10 mm, has a sensitivity rate for the detection of LN metastasis in endometrial cancer between 27 and 66 %, and a corresponding specificity rate between 73 and 99 % [27–32]. In uterine cervical cancer, LN metastasis detection by these methods is between 30 and 73 % sensitive and between 44 and 93 % specific [14, 31, 33–37]. However, PET/CT shows low sensitivity and high specificity for detecting metastatic LNs in patients with uterine cervical and endometrial cancer, whereas DWI shows high sensitivity and low specificity [38].

DWI is an MRI technique that depicts molecular diffusion, which is the Brownian motion of water protons in biological tissues. It has been used in oncological imaging for the depiction and characterization of tumors, as well as for differentiating benign from malignant lesions in various kinds of tumors, including uterine cancer [13, 39]. The extent of water diffusion can be related to microstructure, microcirculation, cell organization and density, thereby enabling DWI to provide information about the biophysical properties of tissues in vivo. Assuming that malignant tumors generally have higher cellularity than benign lesions, DWI might theoretically help in differentiating malignant from benign lesions. However, DWI not only visualizes pathological areas in malignant lesions but also benign pathologies with restricted diffusion [39].

Kitajima et al. [38] reported that DWI shows higher sensitivity and lower specificity than PET/CT in detecting LN metastasis in patients with uterine cancer (endometrial cancer and cervical cancer). However, the quantitative ADC value used is controversial for differentiating malignant from benign LNs in uterine cancer [11–13], suggesting that ADC analysis is not acceptable for the preoperative evaluation of LN metastasis in patients with uterine cancer. This explains why we performed no ADC analyses in our study.

Studies documenting the accuracy of FDG-PET/CT for detecting LN metastasis in uterine cancer [14–20] have reported that PET/CT tends to show low sensitivity and high specificity; this observation is confirmed in our series, and may be explained by the tendency of this technique to underestimate standardized uptake values in tiny LNs due to the partial volume effect. This makes the usual cutoff (2.5–3.0) for differentiating malignant from benign LNs unreliable, and many studies have failed to perform semi-quantitative analysis to determine a standardized value for FDG uptake in nodal lesions [15–17]. FDG-PET/CT is also unable to detect microscopic metastasis, which is unsurprising as PET has a mean spatial resolution value of 0.5 cm (range 0.4–0.6 cm), making small lymph nodal metastases almost undetectable [14–17].

To our knowledge, this is the first reported study to have investigated the validity of retrospectively fused DWI/T2-MRI to PET/CT images from different scanners for nodal staging of endometrial and uterine cervical cancer. All authors have previously focused on the evaluation of conventional MRI (without or with contrast) sequences fused to PET-CT images. For example, Kim et al. [23] showed that the sensitivity and specificity of PET/CT and fused MRI were 44.1 and 93.9 %, and 54.2 and 92.7 %, respectively. The ROC analysis demonstrated a higher diagnostic performance of fused PET/MRI compared to PET/CT alone in the detection of LN metastases ($p = 0.02$). Similarly, Kitajima et al. [24] proved that on a patient basis, the sensitivity, specificity and accuracy for detecting pelvic nodal metastasis were 100, 96.3, and 96.7 % for both fused PET/MRI and PET/contrast-enhanced CT, and 66.7, 100, and 96.7 % for MRI, respectively. The differences between these three parameters were not statistically significant ($p = 1$).

Likewise, we found no statistically significant differences between either PET/CT and MRI-DWI or PET/CT and PET/MRI-DWI on a per-patient basis. We did, however, find that PET/MRI-DWI is as accurate as the most specific and sensitive of the underlying two modalities.

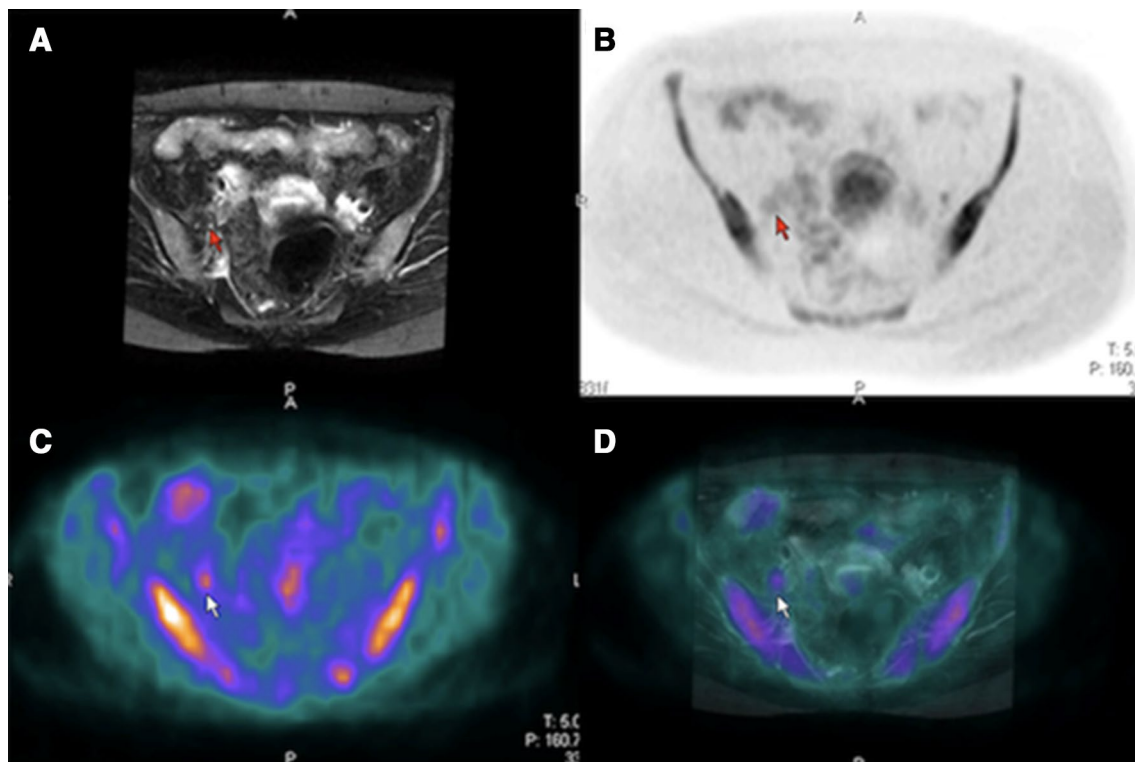


Fig. 3 32-year-old patient with cervical carcinoma. In the T2-weighted MR sequence **a**, **b** there is a slightly hyperintense pathologic tissue (circled in red) in the uterine cervix and bilateral obtura-

tor enlarged lymph nodes (circled in green). DWI **c** and the co-registered PET/DWI images **d** show the same findings

Nevertheless, in our sample there were three false-positives cases with DWI, but true negatives with PET/CT and PET/MRI-DWI. Therefore, DWI shows a lower specificity than PET/CT (68.4 vs 84.2 %). Nonetheless, as shown in Table 4, when the two modalities are fused, there is no difference with PET/CT alone (specificity of PET/DWI-MRI, 84.2 %). However, on a per-node basis, our sensitivity, specificity, PPV and NPV values for fused PET/MRI-DWI were greater than those of PET/CT. This is due to the

high sensitivity of DWI (86.4 %) (Fig. 3) adding to the high specificity of PET/CT (90.5 %) (Figs. 4, 5).

Staging practices vary widely, depending on the individual physician and/or institution. Nevertheless, since the establishment of surgical staging as the standard initial step in the management of most patients with endometrial and cervical cancer, pelvic and para-aortic lymphadenectomy as part of surgical staging has become more common, due to reports showing diagnostic and therapeutic advantages

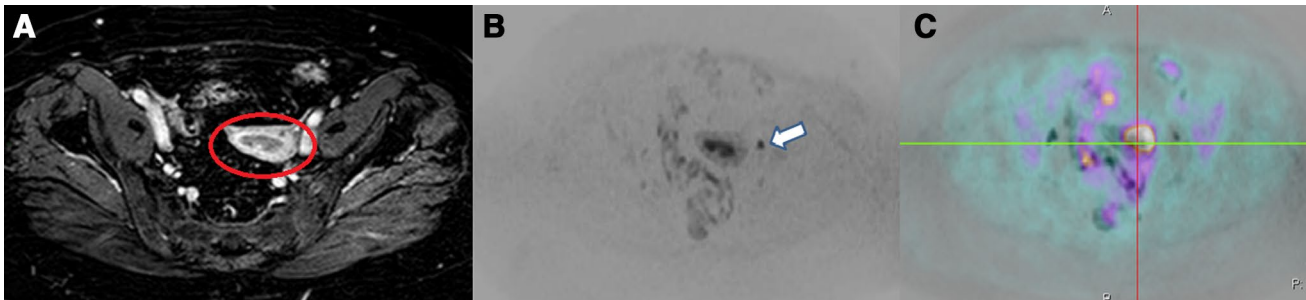


Fig. 4 78-year-old patient with endometrioid carcinoma of uterus. In the THRIVE sequence **a** there is a contrast-enhanced pathological tissue at the uterine corpus-fundus (circled in red). DWI **b** shows a focal area of restriction of diffusivity in the left external iliac loca-

tion (white arrow), scored as possibly metastasis (score 3). The co-registered PET/DWI images **c** do not show any significant uptake in that location (score 0). Surgery confirmed that it was a false positive

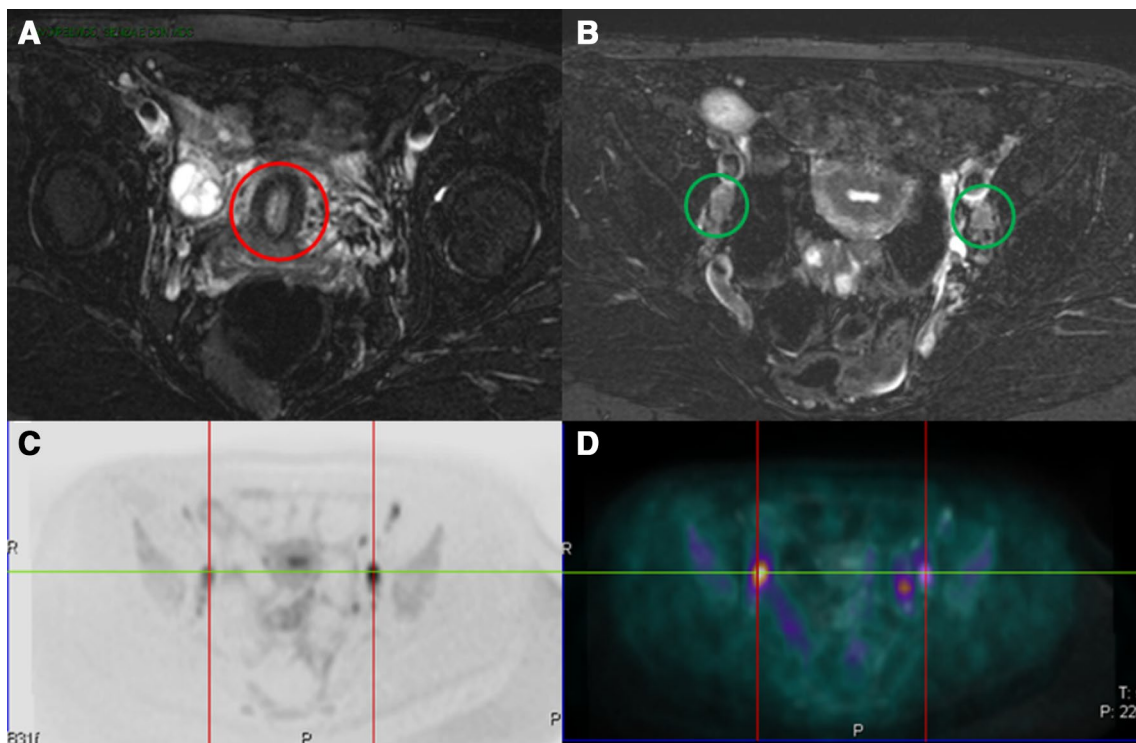


Fig. 5 46-year-old patient with cervical cancer. The T2-weighted MR image **a** shows no pelvic lymph node enlargement. Axial DWI **b** shows a focal area of restriction of diffusivity in the right obturator fossa (red arrow), scored as equivocal (score 2). PET **c** and the

co-registered PET/MRI-DWI images **d** do not show any significant uptake in that location (white arrows). Surgery confirmed that it was a false positive of DWI (bowel loops)

[40–42]. Despite these recommendations, lymph node dissection as a part of endometrial and cervical cancer staging, especially in “low-risk” patients is still controversial. Indeed, nodal resection often does not confer a survival benefit in these patients [43–47], and routine pelvic lymph node dissection may itself expose the patient to risks such as intraoperative vascular injury, as well as, serious complications such as lymphedema and lymphocyst in the long term. Although these risks decrease in the hands of an experienced surgeon [48, 49], the risk of lymphedema and lymphocysts appears to be related to the number of LNs removed [49, 50]. It follows, therefore, that a group of low-risk patients exists who may not need routine lymph node dissection.

In light of our findings, PET/MRI-DWI may prove to be an accurate and non-invasive tool for the pre-planning of surgical procedure and guidance of minimally invasive node resection in low-risk patients. Moreover, PET/MRI-DWI evaluation could be considered in a preoperative prediction model (comprising other parameters such as serum cancer markers, MRI to assess invasion, histological grade, and clinical stage) to determine which patients can avoid lymph node dissection, thereby obviating the need for a pathologist to be present during intraoperative assessment.

However, this study has several limitations. Specifically, our case series was relatively small and a larger number of patients will need to be studied to more accurately evaluate the role of PET/MRI-DWI in LN metastasis detection. Furthermore, in our fused sequences, considering pelvic MR images rather than whole body MRI, we could only assess pelvic, but not para-aortic LNs, whose involvement has nevertheless been assigned an important prognostic value [14, 15]. Moreover, scores were subjective and given by only two readers on the basis of visual interpretation of the images.

Conclusions

Although we found no statistically significant differences between PET/MRI-DWI and PET/CT either on a per-patient or per-node basis, indicating that they have similar diagnostic accuracy in N staging in uterine cancer, PET/MRI-DWI did show higher sensitivity, specificity, PPV and NPV than FDG-PET/CT on a node-by-node basis. Judging by our results, in the absence of other non-invasive N-staging methods for these types of cancer, the potential of imaging fusion techniques deserve further investigation.

Compliance with ethical standards

Conflict of interest The authors declare that they have no conflict of interest.

Ethical standards Informed consent was obtained from all participants. As the study was retrospective, approval of the local ethics committee was not sought.

References

1. Parkin DM, Bray F, Ferlay J et al (2001) Estimating the world cancer burden: globocan 2000. *Int J Cancer* 94:153–156
2. Takeshima N, Yanoh K, Tabata T et al (1999) Assessment of the revised International Federation of Gynecology and Obstetrics staging for early invasive squamous cervical cancer. *Gynecol Oncol* 74:165–169
3. Tanaka Y, Sawada S, Murata T (1984) Relationship between lymph node metastases and prognosis in patients irradiated postoperatively for carcinoma of the uterine cervix. *Acta Radiol Oncol* 23:455–459
4. Downey GO, Potish RA, Adcock LL et al (1989) Pretreatment surgical staging in cervical carcinoma: therapeutic efficacy of pelvic lymph node resection. *Am J Obstet Gynecol* 160:1055–1061
5. Potish RA, Twigg LB, Okagaki T et al (1985) Therapeutic implications of the natural history of advanced cervical cancer as defined by pretreatment surgical staging. *Cancer* 56:956–960
6. Lagasse LD, Creasman WT, Shingleton HM et al (1980) Results and complications of operative staging in cervical cancer: experience of the Gynecologic and Oncology Group. *Gynecol Oncol* 9:90–98
7. Kupets R, Covens A (2001) Is the International Federation of Gynecology and Obstetrics staging system for cervical carcinoma able to predict survival in patients with cervical carcinoma? An assessment of clinimetric properties. *Cancer* 92:796–804
8. Chung CK, Nahhas WA, Zaino R et al (1981) Histologic grade and lymph node metastasis in squamous cell carcinoma of the cervix. *Gynecol Oncol* 12:348–354
9. Van Nagell JR, Roddick JW et al (1971) The staging of cervical cancer: inevitable discrepancies between clinical staging and pathological findings. *Am J Obstet Gynecol* 110:973–978
10. Chan JK, Cheung MK, Huh WK et al (2006) Therapeutic role of lymph node resection in endometrioid corpus cancer: a study of 12,333 patients. *Cancer* 107:1823–1830
11. Kim JK, Kim KA, Park BW et al (2008) Feasibility of diffusion-weighted imaging in the differentiation of meta-static from non-metastatic lymph nodes: early experience. *J Magn Reson Imaging* 28:714–719
12. Nakai G, Matsuki M, Inada Y et al (2008) Detection and evaluation of pelvic lymph nodes in patients with gynecologic malignancies using body diffusion-weighted magnetic resonance imaging. *J Comput Assist Tomogr* 32:764–768
13. Lin G, Ho KC, Wang JJ et al (2008) Detection of lymph node metastasis in cervical and uterine cancers by diffusion-weighted magnetic resonance imaging at 3T. *J Magn Reson Imaging* 28:128–135
14. Choi HJ, Roh JW, Seo SS et al (2006) Comparison of the accuracy of magnetic resonance imaging and positron emission tomography/computed tomography in the presurgical detection of lymph node metastases in patients with uterine cervical carcinoma: a prospective study. *Cancer* 106:914–922
15. Sironi S, Buda A, Picchio M et al (2006) Lymph node metastasis in patients with clinical early-stage cervical cancer: detection with integrated FDG PET/CT. *Radiology* 238:272–279
16. Park JY, Kim EN, Kim DY et al (2008) Comparison of the validity of magnetic resonance imaging and positron emission tomography/computed tomography in the preoperative evaluation of patients with uterine corpus cancer. *Gynecol Oncol* 108:486–492

17. Kitajima K, Murakami K, Yamasaki E et al (2008) Accuracy of 18F-FDG PET/CT in detecting pelvic and paraaortic lymph node metastasis in patients with endometrial cancer. *Am J Roentgenol* 190:1652–1658
18. Kitajima K, Murakami K, Yamasaki E et al (2009) Accuracy of integrated FDG-PET/contrast-enhanced CT in detecting pelvic and paraaortic lymph node metastasis in patients with uterine cancer. *Eur Radiol* 19:1529–1536
19. Chung HH, Park NH, Kim JW et al (2009) Role of integrated PET-CT in pelvic lymph node staging of cervical cancer before radical hysterectomy. *Gynecol Obstet Invest* 67:61–66
20. Signorelli M, Guerra L, Buda A et al (2009) Role of the integrated FDG PET/CT in the surgical management of patients with high risk clinical early stage endometrial cancer: detection of pelvic nodal metastases. *Gynecol Oncol* 115:231–235
21. Herrman KA, Kohan AA, Gaeta MC et al (2013) PET/MRI: applications in clinical imaging. *Curr Radiol Rep* 1:161–176
22. Yankeelova TE, Peterson TE, Abramson RG et al (2012) Simultaneous PET–MRI in oncology: a solution looking for a problem? *Magn Reson Imaging* 30(9):1342–1356
23. Kim SK, Choi HJ, Park SY et al (2009) Additional value of MR/PET fusion compared with PET/CT in the detection of lymph node metastases in cervical cancer patients. *Eur J Cancer* 45:2103–2109
24. Katajima K, Suenaga Y, Ueno Y et al (2013) Value of fusion of PET and MRI for staging of endometrial cancer: comparison with 18F-FDG contrast-enhanced PET/CT and dynamic contrast-enhanced pelvic MRI. *Eur J Radiol* 82:1672–1676
25. Chou HH, Chang TC, Yen TC et al (2006) Low value of 18F-fluoro-2-deoxy-D-glucose positron emission tomography in primary staging of early-stage cervical cancer before radical hysterectomy. *J Clin Oncol* 24(1):123–128
26. Ma SY, See LC, Lai CH et al (2003) Delayed (18)F-FDG PET for detection of paraaortic lymph node metastases in cervical cancer patients. *J Nucl Med* 44(11):1775–1783
27. Hricak H, Rubinstein LV, Gherman GM et al (1991) MR imaging evaluation of endometrial carcinoma: results of an NCI cooperative study. *Radiology* 179:829–832
28. Sugiyama T, Nishida T, Ushijima K et al (1995) Detection of lymph node metastasis in ovarian carcinoma and uterine corpus carcinoma by preoperative computerized tomography or magnetic resonance imaging. *J Obstet Gynaecol* 21:551–556
29. Connor JP, Andrews JI, Anderson B et al (2000) Computed tomography in endometrial carcinoma. *Obstet Gynecol* 95:692–696
30. Manfredi R, Mirk P, Maresca G et al (2004) Local-regional staging of endometrial carcinoma: role of MR imaging in surgical planning. *Radiology* 231:372–378
31. Rockall AG, Sohaib SA, Harisinghani MG et al (2005) Diagnostic performance of nanoparticle enhanced magnetic resonance imaging in the diagnosis of lymph node metastases in patients with endometrial and cervical cancer. *J Clin Oncol* 23:2813–2821
32. Rockall AG, Meroni R, Sohaib SA et al (2007) Evaluation of endometrial carcinoma on magnetic resonance imaging. *Int J Gynecol Cancer* 17:188–196
33. Kim SH, Kim SC, Choi BI et al (1994) Uterine cervical carcinoma: evaluation of pelvic lymph node metastasis with MR imaging. *Radiology* 190:807–811
34. Scheidler J, Hricak H, Yu KK et al (1997) Radiological evaluation of lymph node metastases in patients with cervical cancer. A meta-analysis. *JAMA* 278:1096–1101
35. Hawighorst H, Schoenberg SO, Knapstein PG et al (1998) Staging of invasive cervical carcinoma and of pelvic lymph nodes by high resolution MRI with a phased-array coil in comparison with pathological findings. *J Comput Assist Tomogr* 22:75–81
36. Yang WT, Lam WW, MY Yu, Cheung TH et al (2000) Comparison of dynamic helical CT and dynamic MR imaging in the evaluation of pelvic lymph nodes in cervical carcinoma. *Am J Roentgenol* 175:759–766
37. Reinhardt MJ, Ehrhrit-Braun C, Vogelgesang D et al (2001) Metastatic lymph nodes in patients with cervical cancer: detection with MR imaging and FDG PET. *Radiology* 218:776–782
38. Kitajima K, Yamasaki E, Kaji Y et al (2012) Comparison of DWI and PET/CT in evaluation of lymph node metastasis in uterine cancer. *World J Radiol* 4(5):207–214
39. Kwee TC, Takahara T, Ochiai R et al (2008) Diffusion-weighted whole-body imaging with background body signal suppression (DWIBS): features and potential applications in oncology. *Eur Radiol* 18:1937–1952
40. Fujii S, Matsusue E, Kigawa J et al (2008) Diagnostic accuracy of the apparent diffusion coefficient in differentiating benign from malignant uterine endometrial cavity lesions: initial results. *Eur Radiol* 18:384–389
41. Kilgore LC, Partridge EE, Alvarez RD et al (1995) Adenocarcinoma of the endometrium: survival comparisons of patients with and without pelvic lymph node sampling. *Gynecol Oncol* 56:29–33
42. Mariani A, Webb MJ, Galli L et al (2000) Potential therapeutic role of para-aortic lymphadenectomy in node positive endometrial cancer. *Gynecol Oncol* 76(3):348–356
43. ACOG (2005) Committee on Practice Bulletins. *Manag Endometr Cancer* 65:1–9
44. Chan JK, Cheung MK, Huh WK et al (2006) Therapeutic role of lymph node resection in endometrioid corpus cancer a study of 12,333 patients. *Cancer* 107(8):1823–1830
45. Bernardini MQ, May T, Khalifa MA et al (2009) Evaluation of two management strategies for preoperative grade 1 endometrial cancer. *Obstet Gynecol* 114(1):7–15
46. Kitchener H, Swart AM, Qian Q et al (2009) Efficacy of systematic pelvic lymphadenectomy in endometrial cancer (MRC ASTEC trial): a randomized study. *Lancet* 373(9658):125–136
47. Benedetti Panici P, Basile S, Maneschi F et al (2008) Systematic pelvic lymphadenectomy vs no lymphadenectomy in early-stage endometrial carcinoma: randomized clinical trial. *J Natl Cancer Inst* 100(23):1707–1716
48. Zhou J, Ran J, He ZY et al (2015) Tailoring pelvic lymphadenectomy for patients with stage IA2, IB1, and IIA1 uterine cervical cancer. *J Cancer* 6(4):377–381
49. Todo Y, Yamamoto R, Minobe S et al (2010) Risk factors for postoperative lower-extremity lymphedema in endometrial cancer survivors who had treatment including lymphadenectomy. *Gynecol Oncol* 119(1):60–64
50. Kong TW, Lee KM, Cheong JY et al (2010) Comparison of laparoscopic vs. conventional open surgical staging procedure for endometrial cancer. *J Gynecol Oncol* 21(2):106–111